
Minimal Explanations for Neural Network Predictions

Ouns El Harzli, Bernardo Cuenca Grau, Ian Horrocks
Department of Computer Science, University of Oxford
Oxford, United Kingdom
Correspondance to ouns.elharzli@new.ox.ac.uk

Abstract

Explaining neural network predictions is known to be a challenging problem. In this paper, we propose a novel approach which can be effectively exploited, either in isolation or in combination with other methods, to enhance the interpretability of neural model predictions. For a given input to a trained neural model, our aim is to compute a smallest set of input features so that the model prediction changes when these features are disregarded by setting them to an uninformative baseline value. While computing such minimal explanations is computationally intractable in general for fully-connected neural networks, we show that the problem becomes solvable in polynomial time by a greedy algorithm under mild assumptions on the network’s activation functions. We then show that our tractability result extends seamlessly to more advanced neural architectures such as convolutional and graph neural networks. We conduct experiments to showcase the capability of our method for identifying the input features that are essential to the model’s prediction.

1 Introduction

Deep Neural Networks have experienced unprecedented success in areas such as image analysis, natural language processing, speech recognition, and data science, with systems outperforming humans in a wide range of tasks [30, 23, 31, 38, 41]. As the use of neural models becomes widespread in complex applications, however, task performance is no longer the only driver of system design, and criteria such as safety, fairness, and robustness have gained significant prominence [25].

Improving model interpretability is an important step towards fulfilling these criteria: if models can explain their predictions, it becomes easier to ensure that decisions based on them are safe, fair and robust [49, 37]. As a result, there is growing interest in the development of techniques for interpreting the predictions of trained neural models. This is, however, notoriously challenging, as models are ‘black boxes’ where predictions rely on numeric calculations in high-dimension embedding spaces.

There is no general agreement on the notion of explanation for a neural prediction [19, 1], and a wealth of different approaches have been proposed. *Rule-based methods* generate explanations in the form of logic rules, which are inherently interpretable [10, 12]. *Attribution-based methods* assign a score to input features quantifying their contribution to the prediction relative to an (application-dependent) baseline [45, 44, 5]. *Example-based methods* explain predictions by retrieving training examples that are most similar to the given input [27, 33]. Finally, *perturbation-based methods* generate corrections to an input causing the model to change its output [48, 22, 34, 8]. Each of these methods, however, comes with its own drawbacks. For instance, attribution methods are vulnerable to adversarial attacks since small changes in the input can lead to significant changes on the assigned scores [18, 13, 47].

In this paper, we propose a notion of explanation that can be effectively exploited to enhance the interpretability of neural predictions. Given a baseline representing absence of information and an input to a trained network, our aim is to compute a smallest set of input features so that the

prediction changes when these features are disregarded by setting them to their corresponding baseline value. The minimality requirement ensures that the explanations capture the ‘essence’ of the predictions, thus providing insights on what the models has actually learnt as well as on the reliability of its predictions. In particular, explanations for a trustworthy prediction summarise the input by disregarding genuinely irrelevant features, whereas explanations for brittle and untrustworthy predictions will reveal interesting adversarial examples [46] as justification for the model’s brittleness.

Our approach effectively combines ideas from attribution and perturbation-based methods. As in attribution methods, we introduce an uninformative baseline as reference and, similarly to perturbation methods, our explanations correspond to minimal input corrections with an observable effect. Our notion of explanation is, however, rather different from related perturbation approaches [48, 34, 8, 15, 22] in that the aim is to identify the essence of the prediction by ‘toggling off’ irrelevant features using the baseline. In addition, as we will see, our approach applies to arbitrary neural architectures under very mild restrictions; this is in contrast to perturbation-based approaches restricted to fully-connected networks with ReLU activation [48], Graph Neural Networks [34, 8], or image analysis [15, 22].

Our contributions are as follows. After introducing the notion of a minimal explanation, we focus on fully-connected networks as a starting point and show that computing minimal explanations is an intractable problem. If, however, the non-linear activations of the network are continuous, differentiable almost everywhere and monotonic (as is the case with standard activations) we can show that minimal explanations are computable in polynomial time by a greedy algorithm. To show correctness of our greedy algorithm, we exploit the theoretical properties of the *Integrated Gradients* method [45], thus establishing an interesting connection between our approach and the theory of attribution methods for neural networks; our algorithm, however, does not rely on the application of any such attribution method, and only requires the ability to run the neural network as a black box. We then further generalise our results to more advanced neural architectures such as Convolutional Neural Networks (CNNs) [20, 30] and Graph Neural Networks (GNNs) [21, 26] and show that the problem remains tractable under suitable generalisations of our monotonicity requirements.

We have implemented our approach and conducted experiments on object recognition tasks using fully-connected and convolutional networks. Our results suggest that, in practice, explanations are of small size, can be efficiently computed, and provide interesting insights on the predictions. In addition to enhancing interpretability, the experiments also suggest that our approach can also be exploited for testing robustness of trained networks and generating relevant adversarial examples.

2 Preliminaries

Notation. We let bold-face lowercase letters denote real-valued vectors, and typically use \mathbf{x} for input feature vectors and \mathbf{x}' for baselines. Given vector \mathbf{x} , we use x_i to denote its i -th component. Given vectors $\mathbf{x}, \mathbf{x}' \in \mathbb{R}^n$ and a subset $S \subseteq \{1, \dots, n\}$ of their components, we denote with $\mathbf{x}^{S|\mathbf{x}'}$ the vector obtained from \mathbf{x} by setting each component x_i with $i \in S$ to x'_i . Similarly, we use bold-face capital letters to denote real-valued matrices and, given matrix \mathbf{M} , we denote its (i, j) component as $M_{i,j}$. Finally, given a function $f : \mathbb{R}^n \mapsto \mathbb{R}$, we denote with $(\nabla f)_i$ the i -th component of the gradient of f .

Fully-Connected Neural Networks. A fully-connected neural network (FCN) with $L \geq 1$ layers and input dimension n is a tuple $\mathcal{N} = \langle \{\mathbf{W}^\ell\}_{1 \leq \ell \leq L}, \{\mathbf{b}^\ell\}_{1 \leq \ell \leq L}, \{\sigma^\ell\}_{1 \leq \ell \leq L} \rangle$. For each layer $\ell \in \{1, \dots, L\}$, the integer $d_\ell \in \mathbb{N}$ is the *width* of layer ℓ and we require $d_L = 1$ and define $d_0 = n$; matrix $\mathbf{W}^\ell \in \mathbb{R}^{d_\ell \times d_{\ell-1}}$ is a *weight matrix*; vector $\mathbf{b}^\ell \in \mathbb{R}^{d_\ell}$ is a *bias vector*; and $\sigma^\ell : \mathbb{R} \mapsto \mathbb{R}$ is a polytime-computable *activation function* applied component-wise to vectors.

The application of network \mathcal{N} to an input feature vector $\mathbf{x} \in \mathbb{R}^n$ generates a sequence $\mathbf{x}^1, \dots, \mathbf{x}^L$ of vectors defined as $\mathbf{x}^\ell = \sigma^\ell(\mathbf{h}^\ell)$, where $\mathbf{x}^0 = \mathbf{x}$ and $\mathbf{h}^\ell = \mathbf{W}^\ell \cdot \mathbf{x}^{\ell-1} + \mathbf{b}^\ell$. The result $\mathcal{N}(\mathbf{x})$ of applying \mathcal{N} to \mathbf{x} is the scalar \mathbf{x}^L . Thus, the neural network realises a function $\mathcal{N} : \mathbb{R}^n \mapsto \mathbb{R}$.

We consider the application of neural networks to classification problems. To avoid trivialities, we focus on classifying an input in two classes based on a numeric threshold $t \in \mathbb{R}$. In this setting, the *prediction* of a network \mathcal{N} on input \mathbf{x} is given by the result of comparing $\mathcal{N}(\mathbf{x})$ to the threshold t .

3 Background on Attribution-based Explanation Methods

Attribution methods [45, 44, 39] are a family of explanation techniques which, given as input function $f : \mathbb{R}^n \mapsto \mathbb{R}$, a vector $\mathbf{x} \in \mathbb{R}^n$ and a baseline vector $\mathbf{x}' \in \mathbb{R}^n$, assign a numerical score or contribution $C_i^f(\mathbf{x}, \mathbf{x}')$ to each component $i \in \{1, \dots, n\}$. Attribution methods are often designed to fulfil some (or all) of the following axioms for all functions $\mathbb{R}^n \mapsto \mathbb{R}$ and vectors $\mathbf{x}, \mathbf{x}' \in \mathbb{R}^n$, components $1 \leq i \leq n$ and coefficients $\lambda_1, \lambda_2 \in \mathbb{R}$.

- *Completeness*: $f(\mathbf{x}) - f(\mathbf{x}') = \sum_{j=1}^n C_j^f(\mathbf{x}, \mathbf{x}')$.
- *Zero-contribution*: $C_i^f(\mathbf{x}, \mathbf{x}') = 0$ whenever $f(\mathbf{y}) = f(y_1, \dots, y_{i-1}, z, y_{i+1}, \dots, y_n)$ for each $\mathbf{y} \in \mathbb{R}^n$ and each $z \in \mathbb{R}$.
- *Symmetry*: $C_i^f(\mathbf{x}, \mathbf{x}') = C_j^f(\mathbf{x}, \mathbf{x}')$ if $x_i = x_j$, $x'_i = x'_j$ and $f(y_1, \dots, y_i, \dots, y_j, \dots, y_n) = f(y_1, \dots, y_j, \dots, y_i, \dots, y_n)$ for each $\mathbf{y} \in \mathbb{R}^n$.
- *Linearity*: $C_i^{\lambda_1 f_1 + \lambda_2 f_2}(\mathbf{x}, \mathbf{x}') = \lambda_1 C_i^{f_1}(\mathbf{x}, \mathbf{x}') + \lambda_2 C_i^{f_2}(\mathbf{x}, \mathbf{x}')$.

Completeness ensures that contributions add up to the change in value of the function. Zero-contribution ensures that arguments not influencing the value of the function are assigned 0 as contribution. Symmetry ensures that arguments playing a symmetric role are assigned the same contribution. Finally, linearity ensures that contributions for a function expressed as a linear combination of other functions can be computed as a linear combination of their contributions.

A wide range of attribution-based methods have been proposed. The *Shapley values* method [39] is one of the most popular thanks to its nice properties. Calculating Shapley values is, however, intractable, which has motivated research on approximation techniques [4]. Other popular attribution methods have been designed specifically for neural networks; these include *Layer-wise Relevance Propagation* [7], *DeepLIFT* [40], *Deep Taylor decompositions* [35], and *Saliency Maps* [42, 2, 11, 9].

We exploit the properties of *Integrated Gradients* [45, 6], which is an attribution method applicable to continuous functions that are differentiable almost everywhere. The contribution of each argument i of a such function f for input vector \mathbf{x} and baseline vector \mathbf{x}' is defined as follows:

$$C_i^f(\mathbf{x}, \mathbf{x}') := (x_i - x'_i) \int_0^1 (\nabla f)_i(\mathbf{x}' + \tau(\mathbf{x} - \mathbf{x}')) d\tau. \quad (1)$$

Integrated gradients is the only path-based attribution method satisfying all of the aforementioned axioms [16]. Furthermore, it is well-suited for functions realised by neural networks, which typically satisfy its continuity and differentiability requirements.

4 Hardness of Computing Minimal Explanations

In this section, we first present our notion of a minimal explanation and then show that computing such explanations is an intractable problem for fully-connected neural networks.

Given a trained FCN \mathcal{N} providing a prediction on an input feature vector \mathbf{x} , our notion of a minimal explanation aims at identifying a smallest set of ‘most relevant’ features for the prediction. Similarly to attribution-based methods, we consider an uninformative baseline \mathbf{x}' for comparison where the use of a suitable baseline can be exploited to ‘toggle off’ or disregard certain features; however, while attribution-based methods determine feature relevance by assigning a numeric value to each component of the input \mathbf{x} , our approach is based in the intuition that the most relevant features are those that result in a change of prediction when set to the baseline value.

Definition 1. *Let \mathcal{N} be a FCN with L layers and input dimension n , let t be a numeric threshold, let $\mathbf{x} \in \mathbb{R}^n$ be such that $\mathcal{N}(\mathbf{x}) \geq t$, and let $\mathbf{x}' \in \mathbb{R}^n$ be a baseline vector. An explanation for $\mathcal{N}(\mathbf{x}) \geq t$ relative to \mathbf{x}' is a subset $E \subseteq \{1, \dots, n\}$ satisfying $\mathcal{N}(\mathbf{x}^{E|\mathbf{x}'}) < t$. The size $|E|$ of E is the number of elements it contains. Furthermore, we say that explanation E is minimal if no $E' \subset \{1, \dots, n\}$ such that $|E'| < |E|$ is an explanation for $\mathcal{N}(\mathbf{x}) \geq t$ relative to \mathbf{x}' .*

Note that changing the baseline may lead to a different explanation for the same prediction. In most applications, however, it is easy to identify a natural baseline independent from the input.

We next show that the decision version of our problem is NP-complete. Thus, to identify a minimal explanation, one may need to consider exponentially-many combinations of input features.

Theorem 1. *The following problem is NP-complete: given as input vectors $\mathbf{x}, \mathbf{x}' \in \mathbb{R}^n$, a FCN \mathcal{N} of input dimension n , a numeric threshold t such that $\mathcal{N}(\mathbf{x}) \geq t$, and a natural number $1 \leq k \leq n$, decide whether there exists an explanation for $\mathcal{N}(\mathbf{x}) \geq t$ relative to \mathbf{x}' of size at most k .*

Proof. We show NP-hardness using a reduction from SUBSET-SUM, which is the problem of checking, given as input integers a_1, \dots, a_m and ξ , whether there exists $S \subseteq \{1, \dots, m\}$ such that $\sum_{i \in S} a_i = \xi$. In the context of this proof, let us denote with $\mathbf{0}_m$ the m -dimensional column null vector and with $\mathbf{1}_m$ the m -dimensional column vector with all components equal to 1.

We map an instance a_1, \dots, a_m, ξ of SUBSET-SUM to an instance of our problem in polynomial time by setting $k = m$, $t = 1$, $\mathbf{x} = \mathbf{1}_{m+1}$, $\mathbf{x}' = \mathbf{0}_{m+1}$ and \mathcal{N} to the 3-layer network defined as given next. In the first layer, \mathbf{W}^1 is the identity with dimension $m + 1$ and $\mathbf{b}^1 = \mathbf{0}_{m+1}$; for each $1 \leq i \leq m + 1$, $\sigma_i^1(y)$ is 1 if $y_i = 0$, and 0 otherwise. In the second layer, \mathbf{W}^2 is a $(2 \times m + 1)$ matrix with values $a_1, \dots, a_m, 0$ in the first row and having $\mathbf{1}_{m+1}$ as the second row; furthermore, $\mathbf{b}^2 = \mathbf{0}_2$, $\sigma_1^2(z) = -1$ if $z = \xi$ and $\sigma^2(z) = 1$ otherwise, $\sigma_2^2(z) = 2$ if $z = 0$ and $\sigma_2^2(z) = 1$ otherwise. In the third layer, $\mathbf{W}^3 = \mathbf{1}_2$, $\mathbf{b}^3 = \mathbf{0}$, and $\sigma^3(z) = 1$ if $z \geq 1$ and $\sigma^3(z) = 0$ otherwise. By construction, $\mathcal{N}(\mathbf{x}) \geq 1$, so each valid input to SUBSET-SUM is mapped to a valid input of our problem.

Assume there is an explanation E for $\mathcal{N}(\mathbf{x}) \geq 1$ relative to \mathbf{x}' of size at most $k = m$. By definition, $\mathcal{N}(\mathbf{x}^{E|\mathbf{x}'}) < 1$. We claim that, by construction of \mathcal{N} , E is a solution to the corresponding subset sum instance. Indeed, $\sigma_2^2(h_2^2) \geq 1$ so the only way to have $h^3 < 1$ is to have $\sigma_1^2(h_1^2) = -1$, thus $h_1^2 = \xi$. It follows that E is a solution to $\sum_{i \in E} a_i = \xi$ since, by construction, $h_1^2 = \sum_{i \in E} a_i$.

For the converse, let E be a solution to SUBSET-SUM. We claim that E is also a solution to our problem. Indeed, $m + 1 \notin E$, thus $h_2^2 \neq 0$ and $\sigma_2^2(h_2^2) = 1$. Furthermore, $\sum_{i \in E} a_i = \xi$, thus with input $\mathbf{x}^{E|\mathbf{x}'}$, we have $h_1^2 = \xi$, which gives $\sigma^2(h_1^2) = -1$ and thus $h^3 = 0$, yielding $\mathcal{N}(\mathbf{x}^{E|\mathbf{x}'}) < 1$.

Membership in NP follows since a set $E \subseteq \{1, \dots, n\}$ of size at most k provides a certificate. In particular, E is an explanation if $\mathcal{N}(\mathbf{x}^{E|\mathbf{x}'}) < t$, which is verifiable in polynomial time. \square

The proof of the theorem shows that intractability depends on the dimension of the feature and baseline vectors, but not on their concrete values. Neural networks, however, can have a large number of input features, which makes the computation of minimal explanations problematic. Thus, our focus in the remainder of this paper will be on identifying additional requirements on the trained neural model ensuring that minimal explanations can be computed in polynomial time.

5 Neural Networks with Monotonic Activation

The crucial observation that we can draw from the proof of Theorem 1 is that the activation functions exploited in our reduction are Delta-style functions which are neither continuous nor monotonic. This is in stark contrast with the standard functions used in practice, such as the (different variants of) ReLU, sigmoid or tanh [20]. This observation suggests the following definition of a *monotonic* FCN.

Definition 2. *A fully-connected neural network $\mathcal{N} = \langle \{\mathbf{W}^\ell\}_{1 \leq \ell \leq L}, \{\mathbf{b}^\ell\}_{1 \leq \ell \leq L}, \{\sigma^\ell\}_{1 \leq \ell \leq L} \rangle$ is monotonic if, for each $1 \leq \ell \leq L$, function σ^ℓ is continuous everywhere, differentiable almost everywhere, and monotonic.*

In the remainder of this section we present our main result, which establishes that minimal explanations can be computed in polynomial time for monotonic FCNS by means of a greedy algorithm. As a result, our intractability result in Theorem 1 does not apply to most FCNs used in practice.

5.1 Properties of Monotonic Neural Networks

Consider a trained FCN \mathcal{N} where the activation functions satisfy the requirements in Definition 2. The continuity and differentiability requirements ensure that the gradient of \mathcal{N} can be computed for each input vector \mathbf{x} . In turn, as we show next, the monotonicity requirement ensures that each component of the gradient of \mathcal{N} at \mathbf{x} can be expressed as a sum where (I) the number of elements in the sum is fixed for \mathcal{N} (i.e., it does not depend on \mathbf{x}) and it is the same for all components; and

(2) each element of the sum consists of a product involving a value that depends on \mathbf{x} but which is *always non-negative*, and two coefficients that do not depend on \mathbf{x} .

This key property of the gradient in monotonic FCNs allows us to exploit the theoretical properties of the integrated gradients attribution method. In particular, we can show that, by setting a component of the input vector \mathbf{x} to the baseline, we are not altering the relative order of the integrated gradient attributions (computed as in Equation 1) associated with the remaining components.

These properties, which are established by the following technical lemma, constitute the basis of our greedy algorithm for computing minimal explanations.

Lemma 1. *For each FCN \mathcal{N} with input dimension n , there exists a non-negative integer M , real coefficients $\{A_m\}_{1 \leq m \leq M}$ and $\{B_{m,i}\}_{1 \leq m \leq M, 1 \leq i \leq n}$, and functions $\{g_m\}_{1 \leq m \leq M}$ from \mathbb{R}^n to $\mathbb{R}_{\geq 0}$, such that the following identities are satisfied for each $\mathbf{x}, \mathbf{x}' \in \mathbb{R}^n$ and each $i, j \in \{1, \dots, n\}$:*

$$(\nabla \mathcal{N})_i(\mathbf{x}) = \sum_{m=1}^M A_m B_{m,i} g_m(\mathbf{x}), \quad \text{and} \quad (2)$$

$$\mathcal{N}(\mathbf{x}^{\{i\}|\mathbf{x}'} - \mathbf{x}^{\{j\}|\mathbf{x}'} - \mathbf{x}^{\{i\}|\mathbf{x}'} + \mathbf{x}^{\{j\}|\mathbf{x}'} = \sum_{m=1}^M A_m (B_{m,i}(x'_i - x_i) - B_{m,j}(x'_j - x_j)) \int_0^1 g_m(\mathbf{p}^{ij}(\tau)) d\tau \quad (3)$$

where $\mathbf{p}^{ij}(\tau) = \mathbf{x}^{\{j\}|\mathbf{x}'} + \tau(\mathbf{x}^{\{i\}|\mathbf{x}'} - \mathbf{x}^{\{j\}|\mathbf{x}'}).$

Proof. We show (2) by induction on the number L of layers in \mathcal{N} . If $L = 1$, then $\mathcal{N} = \langle \mathbf{W}, b, \sigma \rangle$ with \mathbf{W} an n -dimensional vector, b a scalar and $\sigma : \mathbb{R} \mapsto \mathbb{R}$. Using the chain rule, we have $(\nabla \mathcal{N})_i(\mathbf{x}) = W_i \cdot (D\sigma)(\mathbf{W} \cdot \mathbf{x} + b)$, where $D\sigma$ is the derivative of σ in Euler's notation. This expression is of the form (2) with $M = 1$, $B_{1,i} = W_i$, $A_1 = 1$ if σ is monotonically increasing (dually, $A_1 = -1$ if σ is monotonically decreasing), and $g_1(\mathbf{x}) = (D\sigma)(\mathbf{W} \cdot \mathbf{x} + b)$ if σ is monotonically increasing (dually, $g_1 = -(D\sigma)(\mathbf{W} \cdot \mathbf{x} + b)$ if σ is monotonically decreasing). In both cases, monotonicity of σ ensures that $g_1(\mathbf{x}) \geq 0$ for any \mathbf{x} .

For the inductive case, assume that (2) holds for every network with $L - 1$ layers. The application of $\mathcal{N} = \langle \{\mathbf{W}^\ell\}_{1 \leq \ell \leq L}, \{\mathbf{b}^\ell\}_{1 \leq \ell \leq L}, \{\sigma^\ell\}_{1 \leq \ell \leq L} \rangle$ with L layers to an input \mathbf{x} is defined as $\sigma^L(h^L(\mathbf{x}))$. Thus, we can apply the chain rule and the definition of h^L to obtain the following identity:

$$(\nabla \mathcal{N})_i(\mathbf{x}) = (\nabla h^L)_i(\mathbf{x}) \cdot (D\sigma^L)(h^L(\mathbf{x})) = \sum_{j=1}^{d_{L-1}} W_j^L \cdot (\nabla \mathcal{N}^j)_i(\mathbf{x}) \cdot (D\sigma^L)(h^L(\mathbf{x})). \quad (4)$$

Here, \mathcal{N}^j is specified by $\langle \{\mathbf{W}^\ell\}_{1 \leq \ell \leq L-2}, \mathbf{W}_j^{L-1}, \{\mathbf{b}^\ell\}_{1 \leq \ell \leq L-2}, b_j^{L-1}, \{\sigma^\ell\}_{1 \leq \ell \leq L-1} \rangle$, where \mathbf{W}_j^{L-1} and b_j^{L-1} are the j -th row of \mathbf{W}^{L-1} and the j -th element of \mathbf{b}^{L-1} , respectively.

We now apply the inductive hypothesis to obtain the value of the gradient for each $1 \leq j \leq d_L - 1$, which is given by $(\nabla \mathcal{N}^j)_i(\mathbf{x}) = \sum_{m_j=1}^{M_j} A_{m_j}^j B_{m_j,i}^j g_{m_j}^j(\mathbf{x})$. But now, we can replace the value of the gradients in the sum of equation (4) with these values and directly show the statement of the lemma by instantiating equation (2) with $M = \sum_{j=1}^{d_{L-1}} M_j$, $A_m = \pm W_j^L A_{m_j}^j$, $B_{m,i} = B_{m_j,i}^j$ and $g_m(\mathbf{x}) = \pm g_{m_j}^j(\mathbf{x}) \cdot (D\sigma^L)(h^L(\mathbf{x}))$, where the sign in \pm is determined by whether σ is monotonically increasing or decreasing. Again, it follows that $g_m(\mathbf{x}) \geq 0$ for each m and \mathbf{x} .

We now show Equation (3). Let us consider the attribution for \mathcal{N} defined in (1). Assume $i \neq j$ (otherwise the equation holds trivially). By replacing the value of the gradient in (1) with (2), we obtain $C_i^{\mathcal{N}}(\mathbf{x}, \mathbf{x}') = \sum_{m=1}^M A_m B_{m,i}(x_i - x'_i) \int_0^1 g_m(\mathbf{x}' + \tau(\mathbf{x} - \mathbf{x}')) d\tau$. Since integrated gradients satisfy the completeness and zero contribution axioms, we can compute the difference $\mathcal{N}(\mathbf{x}^{\{i\}|\mathbf{x}'} - \mathbf{x}^{\{j\}|\mathbf{x}'} - \mathbf{x}^{\{i\}|\mathbf{x}'} + \mathbf{x}^{\{j\}|\mathbf{x}'} as the sum of contributions $C_i^{\mathcal{N}}(\mathbf{x}^{\{i\}|\mathbf{x}'} - \mathbf{x}^{\{j\}|\mathbf{x}'})$ and $C_j^{\mathcal{N}}(\mathbf{x}^{\{i\}|\mathbf{x}'} - \mathbf{x}^{\{j\}|\mathbf{x}'})$ to obtain $(x'_i - x_i) \int_0^1 (\nabla \mathcal{N})_i(\mathbf{p}^{ij}(\tau)) d\tau - (x'_j - x_j) \int_0^1 (\nabla \mathcal{N})_j(\mathbf{p}^{ij}(\tau)) d\tau$. Equation (2) provides the values for the gradients $(\nabla \mathcal{N})_i(\mathbf{p}^{ij}(\tau))$ and $(\nabla \mathcal{N})_j(\mathbf{p}^{ij}(\tau))$, which we can replace in the previous expression to finally derive Equation (3). $\square$$

Algorithm 1

Input: monotonic FCN \mathcal{N} , vectors $\mathbf{x}, \mathbf{x}' \in \mathbb{R}^n$ and threshold $t \in \mathbb{R}$ such that $\mathcal{N}(\mathbf{x}) \geq t$.
for $1 \leq j \leq n$ **do**
 $c_j \leftarrow \mathcal{N}(\mathbf{x}^{\{j\}|\mathbf{x}'})$
end for
 $I \leftarrow$ list of indices obtained from sorting $\{c_j\}_{1 \leq j \leq n}$ in ascending order with ties broken arbitrarily.
 $E \leftarrow \emptyset$
for $1 \leq j \leq n$ **do**
 $E \leftarrow E \cup I[j]$
 if $\mathcal{N}(\mathbf{x}^{E|\mathbf{x}'}) < t$ **then return** E
end for

5.2 A Greedy Algorithm for Computing Minimal Explanations

In this section, we propose a greedy algorithm for computing a minimal explanation for a given prediction of a monotonic FCN.

Algorithm 1 proceeds as detailed next. In each iteration of the first loop, the algorithm sets each individual input feature to the baseline value (while leaving the remaining components unchanged) and applies the input FCN to the resulting vector. The values obtained by each of these applications of the FCN are then sorted in ascending order. In the second loop, the algorithm successively sets the components of \mathbf{x} to the baseline in the order established in the previous step until the prediction no longer holds. The algorithm then returns E consisting of all features that were set to the baseline. Our algorithm is quadratic in the number of input features: both loops require linearly many applications of the FCN, and each application is feasible in linear time in the number of features [20]. The algorithm’s correctness relies on Equation (3) in Lemma 1, which ensures that, when set to the baseline, each of the features selected by the algorithm in the second loop yields the largest change (amongst all other possible feature choices) in the evaluation of the network, thus bringing the network’s output as close as possible to the prediction threshold. As a result, the output explanation E is guaranteed to contain a smallest number of features.

Theorem 2. *Algorithm 1 computes a minimal explanation for $\mathcal{N}(\mathbf{x}) \geq t$ relative to \mathbf{x}' .*

Proof. It suffices to show that, for each $j \in \{1, \dots, n\}$, the choice of $I[j]$ in the second loop yields the largest change in the evaluation of \mathcal{N} . That is, for each $1 \leq j \leq n$ and $j \leq k \leq n$ we have $\mathcal{N}(\mathbf{x}^{E|\mathbf{x}'}) - \mathcal{N}(\mathbf{x}^{(E \cup I[j])|\mathbf{x}'}) \geq \mathcal{N}(\mathbf{x}^{E|\mathbf{x}'}) - \mathcal{N}(\mathbf{x}^{(E \cup I[k])|\mathbf{x}'})$. By construction of list I , the inequality $\mathcal{N}(\mathbf{x}^{I[j]|\mathbf{x}'}) - \mathcal{N}(\mathbf{x}^{I[k]|\mathbf{x}'}) \leq 0$ holds for each $1 \leq j \leq k \leq n$. We apply Equation (3) in Lemma 1 together with the fact that $g_m(\mathbf{x}) \geq 0$ for each m and \mathbf{x} (and hence $\int_0^1 g_m(\mathbf{p}^{ij}(\tau)) d\tau \geq 0$) to obtain $\sum_{m=1}^M A_m (B_{m,I[j]}(x'_{I[j]} - x_{I[j]}) - B_{m,I[k]}(x'_{I[k]} - x_{I[k]})) \leq 0$. Since $\{I[j], I[k]\} \subseteq \{1, \dots, n\} - E$, we have $(\mathbf{x}^{E|\mathbf{x}'})_{I[j]} = x_{I[j]}$ and $(\mathbf{x}^{E|\mathbf{x}'})_{I[k]} = x_{I[k]}$. By applying Equation (3) and the previous inequality, we obtain $\mathcal{N}((\mathbf{x}^{E|\mathbf{x}'})^{I[j]|\mathbf{x}'}) \leq \mathcal{N}((\mathbf{x}^{E|\mathbf{x}'})^{I[k]|\mathbf{x}'})$. Since $\mathbf{x}^{(E \cup I[j])|\mathbf{x}'} = (\mathbf{x}^{E|\mathbf{x}'})^{I[j]|\mathbf{x}'}$, we finally obtain $\mathcal{N}(\mathbf{x}^{(E \cup I[j])|\mathbf{x}'}) \leq \mathcal{N}(\mathbf{x}^{(E \cup I[k])|\mathbf{x}'})$. \square

Note that, although the correctness of our algorithm relies on the properties of integrated gradients, the algorithm itself only relies on the ability to apply the input network as a ‘black box’ and hence does not involve the computation of any attribution values.

6 Generalisation to Convolutional and Graph Neural Networks

In this section, we generalise our approach to more advanced neural architectures. Our main result is that, under mild monotonicity assumptions, Algorithm 1 continues to work verbatim if the input network \mathcal{N} is a standard Convolutional (or Graph) Neural Network. In particular, we require that the non-linearities in \mathcal{N} can be equivalently expressed as vector fields that are continuous, differentiable almost everywhere and with a Jacobian that is either at least 0 everywhere or at most 0 everywhere;

the latter is the natural generalisation of the monotonicity requirement to vector fields, and it is satisfied by the standard non-linearities included in practical neural architectures.

To establish this result, we start by introducing as a theoretical tool the notion of a *generalised FCN*, where activation functions are defined as vector fields (and hence are no longer restricted to scalar functions applied component-wise to vectors). As discussed later on, this will give us the flexibility needed to mathematically capture the application of CNNs as well as certain variants of GNNs.

Definition 3. A generalised FCN (GFCN) with $L \geq 1$ layers and input dimension $n \in \mathbb{N}$ is a tuple $\mathcal{N} = \langle \{\mathbf{W}^\ell\}_{1 \leq \ell \leq L}, \{\mathbf{b}^\ell\}_{1 \leq \ell \leq L}, \{\sigma^\ell\}_{1 \leq \ell \leq L} \rangle$. For each $\ell \in \{1, \dots, L\}$, integers $d_\ell \in \mathbb{N}$ and $D_\ell \in \mathbb{N}$ represent the width and the pre-activation width of layer ℓ , respectively; we require $d_L = 1$ and define $d_0 = n$; matrix $\mathbf{W}^\ell \in \mathbb{R}^{D_\ell \times d_{\ell-1}}$ is a real-valued weight matrix; vector $\mathbf{b}^\ell \in \mathbb{R}^{D_\ell}$ is the bias vector; and the activation function $\sigma^\ell : \mathbb{R}^{D_\ell} \mapsto \mathbb{R}^{d_\ell}$ is a polytime-computable vector field.

The application of a GFCN \mathcal{N} to a vector $\mathbf{x} \in \mathbb{R}^n$ is defined as given in the preliminaries for FCNs.

The monotonicity requirement for FCNs can be seamlessly lifted to GFCNs, by establishing the natural requirements on the Jacobian of the each activation function in the network. In particular, we require the values of the Jacobian to be either non-negative everywhere or at most 0 everywhere.

Definition 4. A GFCN $\mathcal{N} = \langle \{\mathbf{W}^\ell\}_{1 \leq \ell \leq L}, \{\mathbf{b}^\ell\}_{1 \leq \ell \leq L}, \{\sigma^\ell\}_{1 \leq \ell \leq L} \rangle$ is monotonic if, for each layer $1 \leq \ell \leq L$, the Jacobian \mathbf{J}^ℓ of $\sigma^\ell : \mathbb{R}^{D_\ell} \mapsto \mathbb{R}^{d_\ell}$ satisfies one of the following properties:

- $(\mathbf{J}^\ell(\mathbf{y}))_{ij} \geq 0$ for each $1 \leq i \leq d_\ell$, each $1 \leq j \leq D_\ell$, and each vector $\mathbf{y} \in \mathbb{R}^{D_\ell}$, OR
- $(\mathbf{J}^\ell(\mathbf{y}))_{ij} \leq 0$ for each $1 \leq i \leq d_\ell$, each $1 \leq j \leq D_\ell$, and each vector $\mathbf{y} \in \mathbb{R}^{D_\ell}$.

We next show that Algorithm 1 remains correct if the input network is a monotonic GFCN. This is so because the generalised monotonicity requirement in Definition 4 ensures that Equation (2) in Lemma 1 remains true if \mathcal{N} is a monotonic GFCN.

Theorem 3. Algorithm 1 computes a minimal explanation for $\mathcal{N}(\mathbf{x}) \geq t$ relative to \mathbf{x}' when applied to a monotonic GFCN \mathcal{N} , vectors $\mathbf{x}, \mathbf{x}' \in \mathbb{R}^n$ and threshold $t \in \mathbb{R}$ such that $\mathcal{N}(\mathbf{x}) \geq t$.

Proof. It suffices to show that the statement in Lemma 1 also holds if \mathcal{N} is a GFCN and, in particular, that Equation (2) remains true. To this end, we set up a similar induction on the number L of layers in \mathcal{N} as we did in the proof of Lemma 1. If \mathcal{N} has a single layer ($L = 1$), then $\mathcal{N} = \langle \mathbf{W}, b, \sigma \rangle$, with \mathbf{W} an $(D_1 \times n)$ -matrix, b an D_1 -dimensional vector and σ a scalar field $\sigma : \mathbb{R}^{D_1} \mapsto \mathbb{R}$. By the chain rule, each component of the gradient of \mathcal{N} is given by $(\nabla \mathcal{N})_i(\mathbf{x}) = \sum_{j=1}^{D_1} W_{i,j}^1 (\mathbf{J}^1(\mathbf{W}^1 \cdot \mathbf{x} + b^1))_{1,j}$, where \mathbf{J}^1 is the Jacobian of σ^1 which, in this case, is a row vector. This expression is of the form (2) with $M = D_1$, $A_m = \pm 1$, $B_{m,i} = W_{i,j}^1$ and $g_m(\mathbf{x}) = \pm (\mathbf{J}^1(\sigma^1(\mathbf{W}^1 \cdot \mathbf{x} + b^1)))_{1,j}$ where the sign \pm is chosen depending on the type of monotonicity of the Jacobian (c.f. Definition 4). Observe that $g_m(\mathbf{x}) \geq 0$ by the monotonicity assumption from Definition 4.

For the inductive case, assume that (2) holds for every GFCN with $L - 1$ layers. The application of \mathcal{N} with L layers to \mathbf{x} is given by $\mathcal{N}(\mathbf{x}) = \sigma^L(\mathbf{h}^L(\mathbf{x}))$; thus, by the chain rule, each component of the gradient $(\nabla \mathcal{N})_i$ is now given as the sum $\sum_{j=1}^{D_L} \sum_{k=1}^{d_{L-1}} W_{k,j}^L (\nabla \mathcal{N}^k)_i(\mathbf{x}) (\mathbf{J}^L(\mathbf{h}^L(\mathbf{x})))_{1,j}$. Here, $\mathcal{N}^k = \langle \{\mathbf{W}^\ell\}_{1 \leq \ell \leq L-1}, \{\mathbf{b}^\ell\}_{1 \leq \ell \leq L-1}, \{\sigma^\ell\}_{1 \leq \ell \leq L-2}, \sigma_k^{L-1} \rangle$, where $\sigma_k^{L-1} : \mathbb{R}^{D_{L-1}} \mapsto \mathbb{R}$ is the k -th component of the vector field $\sigma^{L-1} : \mathbb{R}^{D_{L-1}} \mapsto \mathbb{R}^{d_{L-1}}$.

Following the proof of Lemma 1, the application of the inductive hypothesis to GFCN \mathcal{N}^k yields $(\nabla \mathcal{N}^k)_i(\mathbf{x}) = \sum_{m_k=1}^{M_k} A_{m_k}^k B_{m_k,i}^k g_{m_k}^k(\mathbf{x})$. As a result, $(\nabla \mathcal{N})_i$ can be put into form (2) by taking $M = \sum_{j=1}^{D_L} \sum_{k=1}^{d_{L-1}} M_k$, $A_m = \pm A_{m_k}^k W_{k,j}^L$, $B_{m,i} = B_{m_k,i}^k$, and $g_m(\mathbf{x}) = \pm g_{m_k}^k(\mathbf{x}) \cdot (\mathbf{J}^L(\mathbf{h}^L(\mathbf{x})))_{1,j}$. The latter is again non-negative by assumption on the Jacobian. \square

We finally argue that GFCNs are powerful enough to capture CNNs (and certain variants of GNNs) in a way that ensures correctness of Algorithm 1 when applied directly to such neural architectures, provided that their non-linearities satisfy our monotonicity requirements.

Consider a CNN \mathcal{C} and a fixed dimension of input images. We argue that there is a GFCN \mathcal{N} simulating the application of \mathcal{C} to any image with the given dimensions. Thus, correctness of Algorithm 1 applied

to \mathcal{C} is implied by the correctness of the algorithm applied to \mathcal{N} stated in Theorem 3. To see this, first note that the application of convolutional filters within a layer can be simulated by matrix multiplication [20]. In turn, pooling operations can be seen as non-linearities returning a vector of smaller dimension, hence the definition of σ^ℓ as a vector field. Batch normalisation in inference mode can be seen as a linear transformation. Finally, pooling operations composed with standard non-linear activation functions can be simulated by first applying pooling, then multiplying by the identity matrix, and finally applying the standard activation function.

Similarly, GFCNs can also capture basic graph neural networks for which the feature update function is defined as $h_u^\ell = \sigma \left(\sum_{v \in \mathcal{N}(u) \cup \{u\}} \mathbf{W}^\ell h_v^{\ell-1} \right)$, where h_u^ℓ denotes the vector of features of node u at layer ℓ , and $\mathcal{N}(u)$ denotes the neighbours of node u in the input graph. We argue that, given such GNN \mathcal{G} and a fixed topology of input graphs (i.e., a fixed set of nodes, edges, and fixed dimensions of the feature vector associated to each node), there exists a GFCN \mathcal{N} simulating the application of \mathcal{G} to any graph with the given topology. To see this, note that one can flatten the input so that each component of the input space corresponds to a feature of a particular node. The aggregation over neighbourhoods can be captured by matrix multiplication where the matrix has zeros where the corresponding nodes are not in the same neighbourhood, and the matrix has the corresponding weight values where the nodes are in the same neighbourhood. The non-linear activation function is then applied component-wise to each node feature, so it can be reproduced by applying the activation function component-wise to each component of the transformed input. This correspondence also generalises to Graph Convolutional Networks (GCNs) [26]. We note, however, that GFCNs cannot adequately capture arbitrary message-passing GNNs since there exists aggregation functions which cannot be simulated by matrix multiplication followed by the application of a non-linear map.

As a result, we can conclude that our greedy algorithm can be directly applied to CNNs and GNNs commonly used in practice by simply using the networks as a ‘black box’ (and hence without the need of explicitly constructing the corresponding GFCN). In particular, the non-linearities used in practice (max-pooling, average-pooling, ReLU, sigmoid, tanh, softmax, log-softmax) satisfy our requirements.

7 Evaluation

We have implemented Algorithm 1 and applied it to object recognition tasks on the MNIST [32] and CIFAR10 [29] datasets. Image analysis tasks are a natural choice in our setting since explanations can be assessed by inspection of the relevant images. Our approach, however, is applicable to arbitrary classification and regression tasks provided that the neural architecture satisfies our requirements.

Experiments. Using PyTorch [36], we have trained an FCN with ReLU and log-softmax activation functions on MNIST using the default split to an accuracy of 97% on the test set. We then used transfer learning to train a VGG16 [43] deep convolutional network with ReLU activation functions and max-pooling on CIFAR10 using the default split to an accuracy of 92% on the test set.

We then applied Algorithm 1 to each of these trained networks and each of the examples in the test set of the relevant benchmark using the standard baseline in attribution-based methods for image analysis [45]. For comparison, we used the Captum implementation [28] to compute attributions based on integrated gradients for each network and relevant test image using the same standard baseline.

All experiments were conducted on GPU on Google Colab.

Results and Discussion. Minimal explanations computed by Algorithm 1 using our trained FCN on the MNIST test contained on average 29 out of 784 pixels (3.6% of the image) and took 2.4 seconds per prediction on average to compute. In turn, minimal explanations using VGG16 on CIFAR10 contained 119 out of 3072 features on average (3.9%) and took 65s on average to compute.

Figures 1 and 2 depict a selection of results on MNIST and CIFAR10 test examples, respectively. For each example, we provide three images: the image on the left is the original test image, the middle one represents the modified image where the pixels in the computed minimal explanation have been removed, and the image on the right depicts a heat map based on the attributions computed using integrated gradients. In the case of CIFAR10, our algorithm can modify the color of a pixel by setting only one or some of the RGB components to the baseline.

We can classify the examples in Figure 1 into 2 groups. In the first group, the explanation intuitively captures the essence of the prediction and the resemblance between the middle image and the modified

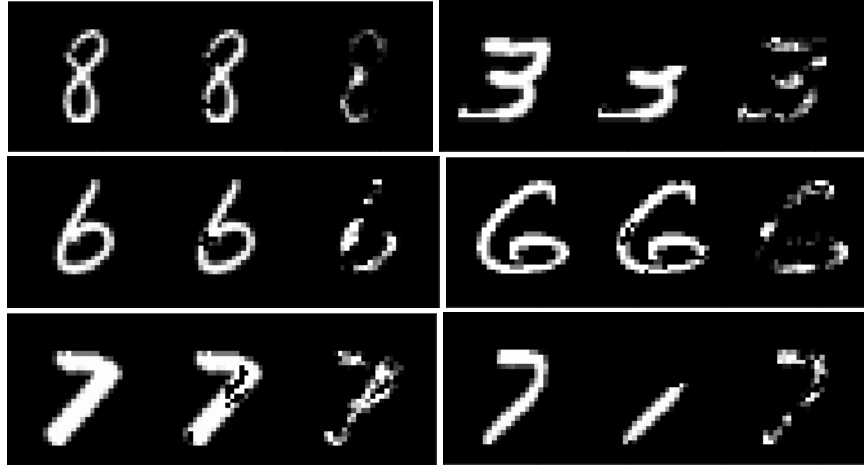


Figure 1: Sample results on MNIST

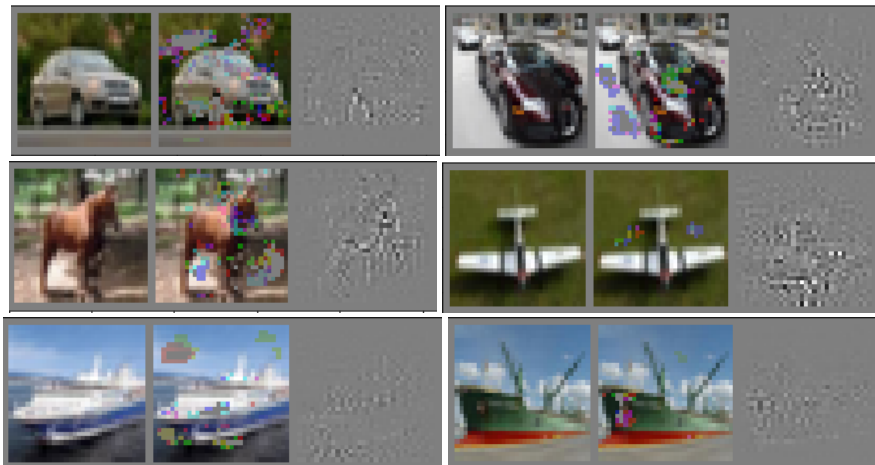


Figure 2: Sample results on CIFAR10.

prediction is apparent. For instance, the modified "3" on the top right example is classified as "5", the modified "6" on the left example of the second row is classified as "5" and the modified "8" on the top left example is classified as "3". In contrast, in the second group, the explanation suggests the vulnerability of the model against adversarial attacks, and the brittleness of its predictions. On the right example in the second row, the modified "6" is classified as "9", and on the left and right examples in the third row, the modified "7"s are classified as "2"s. Interestingly, the heatmap based on integrated gradient attributions does not suggest this important distinction.

The examples in Figure 2 all highlight the brittleness of the predictions. The modified car on the top left is classified as a bird and the one on the top right is classified as a frog. The modified horse on the second row classified as a truck and the modified plane as a ship. Finally, on the third row, the modified ship on the left is classified as a car and the one on the right as a plane. Again, the integrated gradient attributions do not reveal the brittleness of predictions.

8 Conclusion and Future Work

We have proposed a novel approach for explaining neural predictions which effectively combines ideas from attribution and perturbation-based methods. Our minimal explanations can be efficiently computed for a wide range of neural architectures, and our experiments on image analysis tasks confirm that they provide interesting insights on the reliability of the predictions. In line with existing

work [3, 14, 24], our approach could also be incorporated in the training process to improve network’s robustness; this is so because, for instance, explanations can be used to generate additional training examples.

One limitation of our approach is scalability since our algorithm is quadratic in the number of features; we expect, however, that parallelising predictions can help in that regard. An additional limitation is that explanations will often correspond to adversarial examples if the neural network is not robust enough (especially for multi-class classification where they tend to introduce essential features of a different class). Hence, an interesting direction for future work is to extend our approach to Bayesian neural networks [17], which account for uncertainty when fed out-of-distribution examples.

References

- [1] A. Adadi and M. Berrada. “Peeking Inside the Black-Box: A Survey on Explainable Artificial Intelligence (XAI)”. In: *IEEE Access* 6 (2018), pp. 52138–52160. DOI: 10.1109/ACCESS.2018.2870052.
- [2] J. Adebayo et al. “Sanity Checks for Saliency Maps”. In: *Advances in Neural Information Processing Systems*. Vol. 31. 2018. URL: <https://proceedings.neurips.cc/paper/2018/file/294a8ed24b1ad22ec2e7efea049b8737-Paper.pdf>.
- [3] D. Alvarez Melis and T. Jaakkola. “Towards Robust Interpretability with Self-Explaining Neural Networks”. In: *Advances in Neural Information Processing Systems*. Vol. 31. 2018.
- [4] M. Ancona, C. Oztireli, and M. Gross. “Explaining Deep Neural Networks with a Polynomial Time Algorithm for Shapley Values Approximation”. In: *Proceedings of the 36th International Conference on Machine Learning*. Vol. 72. 2019.
- [5] M. Ancona et al. “Towards better understanding of gradient-based attribution methods for Deep Neural Networks”. In: *International Conference on Learning Representations*. 2018. URL: <https://openreview.net/forum?id=Sy21R9JAW>.
- [6] R. J. Aumann and L.S. Shapley. *Values of Non-Atomic Games*. Princeton University Press, 1974.
- [7] S. Bach et al. “On Pixel-Wise Explanations for Non-Linear Classifier Decisions by Layer-Wise Relevance Propagation”. In: *PLoS ONE* 10 (7 2015).
- [8] M. Bajaj et al. “Robust Counterfactual Explanations on Graph Neural Networks”. In: *Advances in Neural Information Processing Systems*. Vol. 34. 2021.
- [9] C.-H. Chang et al. “Interpreting Neural Network Classifications with Variational Dropout Saliency Maps”. In: *Advances in Neural Information Processing Systems*. Vol. 30. 2017.
- [10] D. J. T. Cucala et al. “Explainable GNN-Based Models over Knowledge Graphs”. In: *International Conference on Learning Representations*. 2022. URL: <https://openreview.net/forum?id=CrCvGNHAIrz>.
- [11] P. Dabkowski and Y. Gal. “Real Time Image Saliency for Black Box Classifiers”. In: *Advances in Neural Information Processing Systems*. Vol. 30. 2017.
- [12] A. Dhurandhar et al. “Explanations based on the missing: Towards contrastive explanations with pertinent negatives”. In: *Advances in Neural Information Processing Systems* 32 (2018).
- [13] A.-K. Dombrowski et al. “Explanations can be manipulated and geometry is to blame”. In: *Advances in Neural Information Processing Systems* 33 (2019).
- [14] G. Erion et al. In: *Nature Machine Intelligence* 3 (2021), 620–631.
- [15] R. C. Fong and A. Vedaldi. “Interpretable Explanations of Black Boxes by Meaningful Perturbation”. In: *Proceedings of the IEEE International Conference on Computer Vision*. 2017.
- [16] E. Friedman. “Paths and consistency in additive cost sharing”. In: *International Journal of Game Theory* 32 (2004), pp. 501–518.
- [17] Y. Gal. “Uncertainty in Deep Learning”. PhD thesis. University of Cambridge, 2016.
- [18] A. Ghorbani, A. Abid, and J. Zou. “Interpretation of Neural Networks Is Fragile”. In: *Thirty-Third AAAI Conference on Artificial Intelligence* (2019).
- [19] L. H. Gilpin et al. “Explaining Explanations: An Overview of Interpretability of Machine Learning”. In: *2018 IEEE 5th International Conference on Data Science and Advanced Analytics*. 2018.

- [20] I. Goodfellow, Y. Bengio, and A. Courville. *Deep Learning*. <http://www.deeplearningbook.org>. MIT Press, 2016.
- [21] M. Gori, G. Monfardini, and F. Scarselli. “A new model for learning in graph domains”. In: *Proceedings of 2005 IEEE International Joint Conference on Neural Networks*. Vol. 2. 2005. DOI: 10.1109/IJCNN.2005.1555942.
- [22] Y. Goyal et al. “Counterfactual Visual Explanations”. In: *Proceedings of the 36th International Conference on Machine Learning*. Vol. 97. 2019, pp. 2376–2384.
- [23] A. Hannun et al. “Deep speech: Scaling up end-to-end speech recognition.” In: *arXiv preprint arXiv:1412.5567* (2014).
- [24] A. A. Ismail, H. Corrada Bravo, and S. Feizi. “Improving Deep Learning Interpretability by Saliency Guided Training”. In: *Advances in Neural Information Processing Systems*. Vol. 34. 2021.
- [25] E. Kazim and A. S. Koshiyama. “A high-level overview of AI ethics”. In: *Patterns* 2 (9 2021). DOI: 10.1016/j.patter.2021.100314.
- [26] T. N. Kipf and M. Welling. “Semi-Supervised Classification with Graph Convolutional Networks”. In: *International Conference on Learning Representations* (2017).
- [27] P. W. Koh and P. Liang. “Understanding black-box predictions via influence functions”. In: *Proceedings of the 34th International Conference on Machine Learning*. Vol. 70. 2017.
- [28] N. Kokhlikyan et al. “Captum: A unified and generic model interpretability library for PyTorch”. In: *arXiv preprint :arXiv:2009.07896* (2020).
- [29] A. Krizhevsky. *Learning multiple layers of features from tiny images*. Tech. rep. 2009.
- [30] A. Krizhevsky, I. Sutskever, and G. E. Hinton. “Imagenet classification with deepconvolutional neural networks.” In: *Advances in Neural Information Processing Systems 25* (2012).
- [31] Y. LeCun, Y. Bengio, and G. Hinton. “Deep learning”. In: *Nature* 521.7553 (2015), pp. 436–444.
- [32] Y. LeCun and C. Cortes. “MNIST handwritten digit database”. In: (2010). URL: <http://yann.lecun.com/exdb/mnist/>.
- [33] O. Li et al. “Deep learning for case-based reasoning through prototypes: A neural network that explains its predictions”. In: *Thirty-Second AAAI Conference on Artificial Intelligence* (2018).
- [34] A. Lucic et al. “CF-GNNExplainer: Counterfactual Explanations for Graph Neural Networks”. In: *Proceedings of The 25th International Conference on Artificial Intelligence and Statistics*. Vol. 151. 2022, pp. 4499–4511.
- [35] G. Montavon et al. “Explaining nonlinear classification decisions with deep Taylor decomposition”. In: *Pattern Recognition* 65 (2017), pp. 211–222. DOI: <https://doi.org/10.1016/j.patcog.2016.11.008>.
- [36] A. Paszke et al. “PyTorch: An Imperative Style, High-Performance Deep Learning Library”. In: *Advances in Neural Information Processing Systems 32*. 2019, pp. 8024–8035.
- [37] W. Samek et al. “Explaining Deep Neural Networks and Beyond: A Review of Methods and Applications”. In: *Proceedings of the IEEE* 109 (3), p. 247. DOI: 10.1109/JPR0C.2021.3060483.
- [38] J. Schmidhuber. “Deep learning in neural networks: An overview”. In: *Neural networks* 61 (2015), pp. 85–117.
- [39] L. Shapley. *Contributions to the Theory of Games II*. Princeton University Press, 1953. Chap. A Value for n-Person Games. DOI: 10.1515/9781400881970-018.
- [40] A. Shrikumar, P. Greenside, and P. Kundaje. “Learning Important Features Through Propagating Activation Differences”. In: *Proceedings of the 34th International Conference on Machine Learning*. Vol. 70. PMLR, 2017, pp. 3145–3153.
- [41] D. Silver et al. “Mastering the game of Go with deep neural networks and tree search.” In: *Nature* 529 (2016).
- [42] K. Simonyan, A. Vedaldi, and A. Zisserman. “Deep Inside Convolutional Networks: Visualising Image Classification Models and Saliency Maps”. In: *International Conference on Learning Representations*. 2014.
- [43] K. Simonyan and A. Zisserman. “Very deep convolutional networks for large-scale image recognition”. In: *arXiv preprint arXiv:1409.1556* (2014).

- [44] M. Sundararajan and A. Najmi. “The Many Shapley Values for Model Explanation”. In: *Proceedings of the 37th International Conference on Machine Learning*. Vol. 119. PMLR, 2020, pp. 9269–9278. URL: <https://proceedings.mlr.press/v119/sundararajan20b.html>.
- [45] M. Sundararajan, A. Taly, and Q. Yan. “Axiomatic Attribution for Deep Networks”. In: *Proceedings of the 34th International Conference on Machine Learning*. Vol. 70. PMLR, 2017, pp. 3319–3328. URL: <https://proceedings.mlr.press/v70/sundararajan17a.html>.
- [46] C. Szegedy et al. “Intriguing properties of neural networks”. In: *International Conference on Learning Representations*. 2014.
- [47] C.-K. Yeh et al. “On the (In)fidelity and Sensitivity of Explanations”. In: *Advances in Neural Information Processing Systems*. Vol. 32. 2019.
- [48] X. Zhang, A. Solar-Lezama, and R. Singh. “Interpreting Neural Network Judgments via Minimal, Stable, and Symbolic Corrections”. In: *Advances in Neural Information Processing Systems*. Vol. 31. 2018.
- [49] Y. Zhang et al. “A Survey on Neural Network Interpretability”. In: *IEEE Transactions on Emerging Topics in Computational Intelligence* 5.5 (2021), pp. 726–742. DOI: 10.1109/TETCI.2021.3100641.